LSD1/KDM1A and GFI1B repress endothelial fate and induce hematopoietic fate in induced pluripotent stem cell-derived hemogenic endothelium

Huan Zhang,[1*] Marten Hansen,[1*] Franca di Summa,[1] Marieke von Lindern,[1] Nynke Gillemans,[2] Wilfred F.J. van Ijcken,[3] Arthur Flohr Svendsen,[1] Sjaak Philipsen,[2] Bert van der Reijden,[4] Eszter Varga[1] and Emile van den Akker[1]

[1]Department of Hematopoiesis, Sanquin Research and Landsteiner Laboratory, Amsterdam; [2]Department of Cell Biology, Erasmus MC, Rotterdam and [3]Center for Biomics, Erasmus MC, Rotterdam and [4]Department of Laboratory Medicine, Laboratory of Hematology, Radboud University Medical Center, Radboud Institute for Molecular Life Sciences, Nijmegen, The Netherlands

HZ and MH contributed equally as first authors.

Correspondence: E. van den Akker
e.vandenakker@sanquin.nl

Received: February 1, 2024.
Accepted: June 24, 2024.
Early view: July 4, 2024.

https://doi.org/10.3324/haematol.2024.285214

Abstract

Differentiation of induced pluripotent stem cells (iPSC) into hematopoietic lineages offers great therapeutic potential. During embryogenesis, hemogenic endothelium (HE) gives rise to hematopoietic stem and progenitor cells through the endothelial-to-hematopoietic transition (EHT). Understanding this process using iPSC is key to generating functional hematopoietic stem cells (HSC), a currently unmet challenge. In this study, we examined the role of the transcriptional factor GFI1B and its co-factor LSD1/KDM1A in EHT. To this end, we employed patient-derived iPSC lines with a dominant-negative dysfunctional *GFI1B* Q287* and irreversible pharmacological LSD1/KDM1A inhibition in healthy iPSC lines. The formation of HE remained unaffected; however, hematopoietic output was severely reduced in both conditions. Single-cell RNA sequencing (scRNAseq) performed on the $CD144^+/CD31^+$ population derived from healthy iPSC revealed similar expression dynamics of genes associated with *in vivo* EHT. Interestingly, LSD1/KDM1A inhibition in healthy lines before EHT resulted in a complete absence of hematopoietic output. However, uncommitted HE cells did not display *GFI1B* expression, suggesting a timed transcriptional program. To test this hypothesis, we ectopically expressed GFI1B in uncommitted HE cells, leading to downregulation of endothelial genes and upregulation of hematopoietic genes, including *GATA2, KIT, RUNX1,* and *SPI1*. Thus, we demonstrate that LSD1/KDM1A and GFI1B can function at distinct temporal points in different cellular subsets during EHT. Although GFI1B is not detected in uncommitted HE cells, its ectopic expression allows for partial hematopoietic specification. These data indicate that precisely timed expression of specific transcriptional regulators during EHT is crucial to the eventual outcome of EHT.

Introduction

During human embryonic development, three spatiotemporally distinct waves of hematopoiesis occur.[1] Each wave exhibits different hematopoietic potencies. Yolk-sac primitive hematopoiesis produces primitive nucleated red blood cells, megakaryocytes, and macrophages.[2] The yolk sac also gives rise to erythroid myeloid progenitors (EMP) that migrate to the fetal liver, generating the first definitive hematopoietic cells (e.g., enucleated red blood cells).[3-5] EMP lack the potential to generate long-term hematopoietic stem cells (LT-HSC) that provide lifelong hematopoietic support.[5,6] LT-HSC arise in the intraembryonic aorta-gonad-mesonephros (AGM) region.[7-10] Both EMP and HSC derive from specialized endothelial cells, or hemogenic endothelium (HE), via a process termed endothelial-to-hematopoietic transition (EHT).[11-15] However, human EHT remains ill-defined due to inaccessibility of primary material. Differentiation of human induced pluripotent stem cells (iPSC) recapitulates certain aspects of embryonic development and provides a feasible model to study early hematopoiesis. Controlling AGM-like EHT from iPSC *in vitro* would be a critical step toward generating an unlimited source of LT-HSC for transplantation purposes and future *in vitro* blood production. So far, *in vitro* production of LT-HSC from iPSC has remained elusive, likely due to the absence of interactions with an

inadequately defined niche and or the inability to capture the correct temporal hematopoietic wave.[1] Interestingly, subcutaneous administration of iPSC into NOD-SCID mice results in teratoma formation, from which CD34$^+$ hematopoietic progenitor cells with long-term repopulating capacity can be isolated.[16] Thus, iPSC lines are intrinsically capable of generating LT-HSC, but current protocols fail to achieve this *in vitro*. Additionally, long-term human hematopoietic reconstitution can be established in mice upon transplanting iPSC-derived HE with overexpression of seven transcription factors (ERG, HOXA5, HOXA9, HOXA10, LCOR, RUNX1, SPI1).[17] Several other transitioning factors and regulators have also been implicated in playing a pivotal role in this process (GFI, GFI1B, RUNX1, GATA2).[18-22]

Runt-related transcription factor 1 (RUNX1) is a key factor in EHT.[23] *Runx1* knockout mice are not viable after embryonic day (E) 12.5 due to a failure to establish adult hematopoiesis.[24,25] Growth factor-independent 1 (GFI1) and growth factor-independent 1B (GFI1B) are RUNX1's downstream targets. They function as transcriptional activators and repressors and share a DNA-binding motif (AATC).[26] GFI1 and GFI1B exert their repressive function by recruiting transcriptional repressor complexes to their N-terminal SNAIL/GFI1 (SNAG) domain.[27] These complexes include lysine specific demethylase LSD1 (KDM1A), histone deacetylase 1 or 2 (HDAC1/2), and REST Corepressor CoREST (RCOR1).[28] They replace active histone modifications with repressive marks, leading to the transcriptional repression of the endothelial program.[29,30] Furthermore, GFI1 and GFI1B can also activate specific genes independent of repressive co-factors recruitment.[31]

Gfi1 knockout results in reduced HSC frequency, and Gfi1b-deficient mice do not develop after E14.5 due to defective erythropoiesis and megakaryopoiesis.[18,19] Deletion of their co-factor, *Lsd1/Kdm1a*, is embryonically lethal (E5.5), while inducible knockdown showed that Lsd1/Kdm1a is essential for maintaining the HSC compartment in adult mice.[32-36] However, the precise function of GFI1B and LSD1/KDM1A on human EHT remains unclear. Although the role of combined overexpression of transcription factors in inducing EHT and trans-differentiation to hematopoietic cells has been studied, it is crucial to understand the contribution of each regulator individually to fully comprehend their role in emerging hematopoiesis from iPSC.

In this study, we aimed to decipher the molecular processes governing human iPSC-derived HE and EHT *in vitro* by manipulating GFI1B and its co-factor LSD1/KDM1A. We present a novel single-cell expression dataset from iPSC-derived HE undergoes EHT, revealing the kinetics of this process and offering insights into the underlying molecular mechanisms. Using a combination of patient-derived iPSC lines carrying a heterozygous mutation (*GFI1B* Q287*) that introduces a stop codon within GFI1B's DNA binding site, inhibitors of LSD1/KDM1A (GSK-LSD1), and overexpression of GFI1B in iPSC-derived HE, we demonstrated that the loss of GFI1B and LSD1/KDM1A function does not impact the generation of HE. However, they are essential for the *in vitro* process of EHT in iPSC.

Methods

Induced pluripotent stem cell culture and differentiation

iPSC lines (*Online Supplementary Appendix*) were maintained on Matrigel (BD Biosciences)-coated plates (TPP) in E8 medium (ThermoFisher Scientific) according to the manufacturer's instructions. Cells were incubated at 37°C with 5% $C0_2$, passaged weekly, and differentiated as described previously.[37] Briefly, iPSC were single-cell seeded on 6 cm Matrigel-coated plates with CloneR (StemCell Technologies) or Revitacell (ThermoFisher Scientific) and cultured for 8 days. When colonies reached a size of 400-600 μm, differentiation was initiated by changing the medium to StemLineII (Sigma) supplemented with 50 ng/mL basic fibroblast growth factor (bFGF) (PeproTech), 40 ng/mL vascular endothelial growth factor (VEGF) (StemCell Technologies), 20 ng/mL BMP4 (PeproTech), and insulin transferrin selenium (ITS, 1:100, ThermoFisher Scientific). At day 6, medium was changed to our homemade CellQuin[38] supplemented with 1:100 ITS, 10 ng/mL VEGF, 20 ng/mL BMP4, 10 ng/mL IL-1β (StemCell Technologies), 1 ng/mL IL-3 (StemCell Technologies), 10 ng/mL IL-6 (StemCell Technologies), 50 ng/mL TPO (StemCell Technologies), and 50 ng/mL stem cell factor (SCF) (culture supernatant from 293T cells expressing ectopic SCF). Where indicated, 4 μM GSK-LSD1 (Sigma) was added to cultures at day 5 or day 6 of iPSC differentiation. Differentiated cells were prepared for flow cytometry analysis at indicated days (*Online Supplementary Appendix; Online Supplementary Table S1*).

Endothelial-to-hematopoietic transition culture and transduction

Hemogenic endothelium (HE) was isolated via magnetic-activated cell sorting (MACS) using CD34 magnetic beads (Miltenyi Biotec). Following the published EHT culture protocol,[17] these cells were maintained on Matrigel-coated plates in serum-free media (StemSpan™ SFEMII, StemCell Technologies) supplemented with 10 μM ROCK inhibitor Y-27632 (StemCell Technologies), 5 ng/mL bFGF, 10 ng/mL BMP4, 5 ng/mL VEGF, 50 ng/mL SCF, 30 ng/mL Nplate (Amgen), 10 ng/mL FLT3 (StemCell Technologies), and 25 ng/mL IGF1 (PeproTech).

293T cells were transfected with either the empty vector (EV) or GFI1B lentiviral construct (*Online Supplementary Appendix*) along with psPAX2 (Addgene #12260) and VSV.G (Addgene #14888) plasmids using Polyethylenimine (PEI, Sigma). After transfection, virus supernatant was collected and applied to CD34$^+$ HE cells. EHT media was refreshed one day post-transduction. Four days later, samples were digested using TrypLE Select (ThermoFisher Scientific) and

prepared for analysis.

Single-cell RNA sequencing analysis

scRNAseq was performed at Single Cell Discoveries (Utrecht, The Netherlands) following standard 10× Genomics 3' V3.1 chemistry protocol. In brief, cells were rehydrated and loaded onto a 10× Chromium controller. Sequencing libraries were prepared following the standard 10× Genomics protocol and sequenced on the Illumina NovaSeq 6000 platform (read length: 150 bp, paired-end). Data analysis was performed with the R packages 'Monocle2' and 'Monocle3'.[39-41] Monocle2 was used for quality control; cells with low or high reads (upper bound 1.3*SD and lower bound 0.3*SD) and mitochondrial contamination were discarded, yielding filtered data. For dimensional reduction, UMAP[42] was used with the following settings: PCA=10, umap.min_dist=0.35, and umap.n.neighbors=5. Cells were clustered using the Leiden algorithm (0.0001 resolution). Trajectory analysis was calculated after UMAP dimensional reduction with a minimal_branch_len of 30 and geodesic_distance_ratio of 1. Differentially expressed genes between clusters were identified using spatial autocorrection analysis, Moran's I, and linear regression model with negative binomial distribution, built within Monocle3.[39-41] Co-regulated genes were grouped into modules using Louvain community analysis[43] and used as inputs for cell type characterization using the Descartes cell types and tissue database.

Bulk RNA sequencing analysis

iPSC-derived HE cells were lentivirally transduced with either EV or GFI1B. RNA library was prepared as previously described[44] and sequenced on the Illumina HiSeq 2500 system. RNA sequencing reads were mapped to GRCh38 (hg38) using STAR. After removing low-quality reads, differential gene expression analysis was conducted using the glmLRT function embedded in the 'edgeR' package in R. We set log2 fold-change at 1 and false discovery rate (FDR) at 0.01.

Gene enrichment analysis

Gene enrichment analysis was conducted using the R package 'clusterProfiler'. Differentially expressed genes were ranked based on the log2 fold-change. These ranked lists were served as input for gene set enrichment analysis (GSEA). We used C2: curated gene sets, C8: cell type signature gene sets, and molecular function (MF) subset of Gene Ontology (GO) gene sets from the Molecular Signatures Database (MSigDB) for GSEA.

Statistics

Statistical analysis was done using GraphPad Prism9 software. Mann-Whitney test or two-way ANOVA, followed by Tukey's multiple comparisons test, were performed. Significance *P* value cutoff was set at 0.05.

Results

An initial wave of CD144$^+$CD309$^+$ endothelial cells precedes the production of hematopoietic cells

In order to study EHT, we established the HE differentiation kinetics using three iPSC control lines obtained from healthy individuals[45,46] and differentiated them toward hematopoietic commitment using our previously established iPSC differentiation protocol (Figure 1A).[37] Cells with both endothelial and hematopoietic potential were defined by the co-expression of CD144 (VE-Cadherin) and CD309 (VEGFR2).[47,48] A gradual decline of CD144$^+$CD309$^+$ cells within the differentiating colonies was observed, decreasing from 18% at day 6 (hematopoietic onset) to 3% at day 11 (Figure 1B). In order to determine whether specification occurred in subsequent differentiation, we further distinguished the CD144$^+$CD309$^+$ population by expression of the endothelial marker CD73 (NT5E) and hematopoietic markers CD43 (SPN) /CD41 (ITGA2B) (*Online Supplementary Figure S1A*). Sorted CD144$^+$CD309$^+$CD73$^+$ cells were adherent cells with endothelial morphology, whereas sorted CD144$^+$CD309$^+$CD41$^+$ cells were suspension cells with blast/hematopoietic morphology. The initial wave of CD144$^+$CD309$^+$ cells was followed by an increase of CD43$^+$ hematopoietic cells in the supernatant (Figure 1C). Hematopoietic suspension cells were distinguished by CD235$^+$ erythroid cells and CD41$^+$ megakaryocytic/hematopoietic progenitor cells (Figure 1D, E). Although heterogeneity was observed between different iPSC lines, the overall differentiation kinetics were similar.

CD144$^+$CD309$^+$ cells intrinsically differentiate toward either endothelial or hematopoietic fate

We then explored whether CD144$^+$CD309$^+$ cells inherently differentiate into either hematopoietic or endothelial cells. We found that CD144$^+$CD309$^+$ cells express CD34, a marker associated with both cell types (Figure 2A). Upon CD34$^+$ enrichment at day 5, before hematopoietic onset, we uncovered the presence of adhering CD144$^+$CD34$^+$CD31$^+$ cells (Figure 2B). These cells were negative for CD73 (mature endothelial marker) and CD43 (hematopoietic marker). However, after an additional 4 days of culture, these cells further differentiated into either CD73$^+$ endothelial cells (68%) or CD43$^+$ hematopoietic cells (19%) with a small percentage (13%) remaining as CD43$^-$CD73$^-$ (Figure 2C, D). These results suggest that once isolated, CD144$^+$CD309$^+$ cells are inherently primed to undergo specification into either hematopoietic or endothelial lineages.

GFI1B and LSD1/KDM1A are essential for hematopoietic specification during endothelial-to-hematopoietic transition from induced pluripotent stem cell

Using the determined iPSC-HE differentiation kinetics as a control, we set out to determine the role of GFI1B and LSD1/KDM1A during *in vitro* EHT from iPSC-HE. We employed two approaches: firstly, we induced EHT in iPSC lines har-

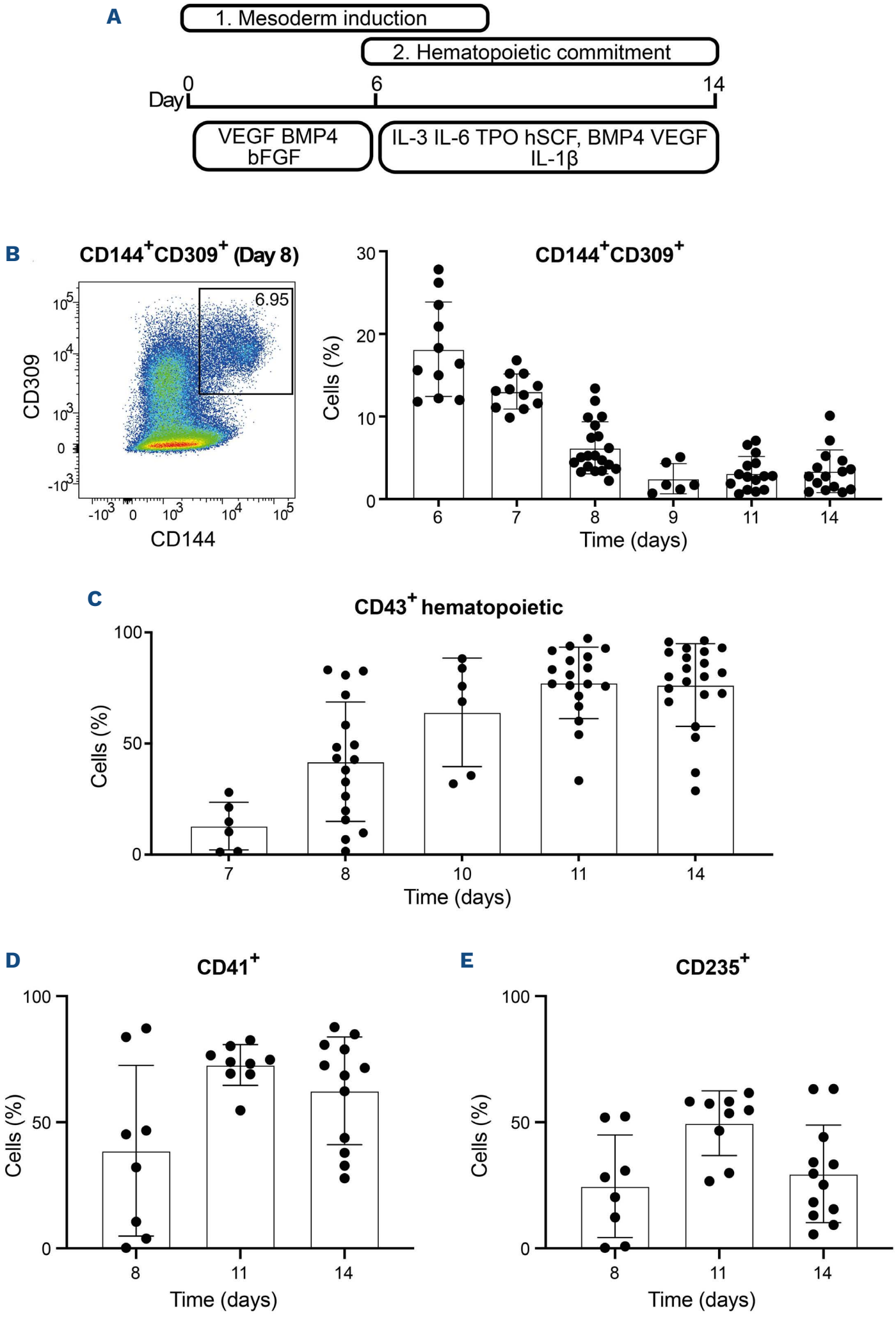

Figure 1. Hematopoietic commitment during induced pluripotent stem cell differentiation. (A) Schematic overview of induced pluripotent stem cell (iPSC) differentiation, specifying stages of induction, the growth factors used, and the differentiation timeline in days.[37] (B) Gating strategy to track hematopoietic/endothelial precursors during iPSC differentiation in culture dish-adherent colonies through assessing the expression of CD144 and CD309. The percentage of $CD144^+CD309^+$ cells from day 6 to 14 during differentiation is shown on the right (mean +/- standard deviation [SD]; N=6-20). (C) Early hematopoietic commitment evaluated by the percentage of $CD43^+$ cells in suspension from day 7 to 14 during iPSC differentiation (mean +/- SD; N=6-21). (D) Percentage of $CD41^+$ megakaryocytic/hematopoietic progenitor cells and (E) $CD235^+$ erythroid cells in suspension at day 8, 11, and 14 of iPSC differentiation (mean +/- SD; N=8-12).

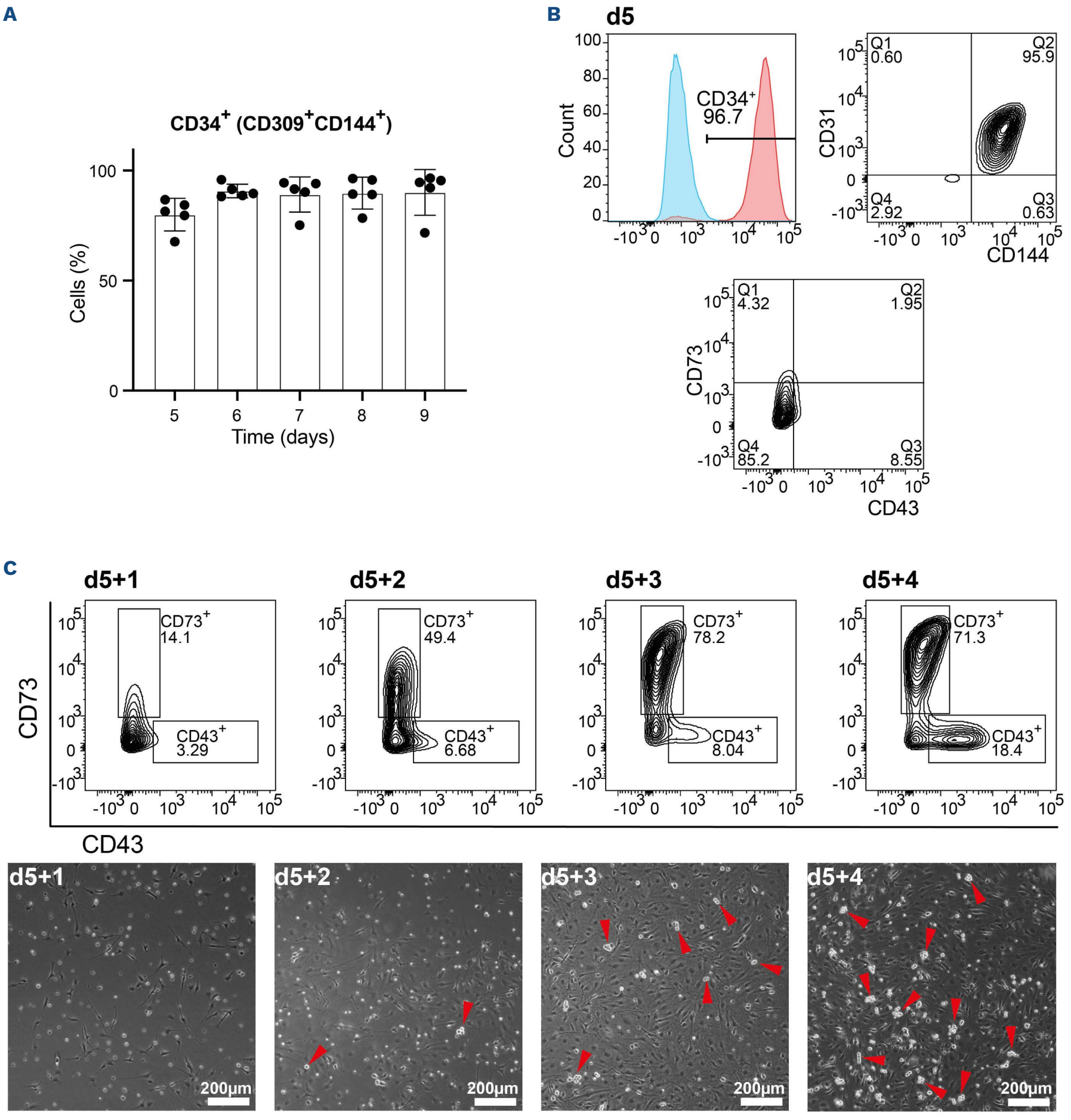

Figure 2. Culture and specification of sorted hematopoietic/endothelial precursors. (A) Proportion of CD34⁺ cells within the CD309⁺CD144⁺ population from day 5 to day 9 during induced pluripotent stem cell (iPSC) differentiation (mean +/- standard deviation [SD]; N=5). (B) CD34 magnetic-activated cell sorting (MACS)-sorted hematopoietic/endothelial precursors on day 5 of iPSC differentiation, with a purity of 96.7% (top left, blue: unstained; red: CD34 staining), highly enriched for CD31 and CD144 (95.9%, top right), predominantly uncommitted or negative for CD43 and CD73 (85.2%). (C) The development of hematopoietic/endothelial cells upon sub-culturing of day 5 CD34⁺ precursors, captured at intervals of 1-, 2-, 3-, and 4-days post-plating. Representative figures showing the morphological progression (scale bar: 200 µm; red arrows indicate examples of the emerging hematopoietic cells). (D) Differentiation of day 5 CD34⁺ precursors into CD73⁺ endothelial (in blue circle) and CD43⁺ hematopoietic (in red square) cells at day 1 and day 4 after sub-culturing. Data represents mean (N=2).

boring the *GFI1B* Q287* dominant-negative mutation.[49,50] Secondly, we pharmacologically inhibited LSD1/KDM1A (GSK-LSD1) at day 6 in control iPSC lines (Figure 3A).[37,45,46] Within the differentiating adherent cells of both *GFI1B* Q287* and GSK-LSD1 conditions, the production and kinetics of CD144+CD309+ cells were not affected (Figure 3B). However, a significant decrease in hematopoietic commitment was observed, evidenced by the reduction of $CD43^+$ cells (Figure 3C). Concurrently, there was an increase in the $CD73^+$ endothelial population in both conditions (*Online Supplementary Figure S1B*). Next, we examined the hematopoietic output, which comprises non-adherent blast cells

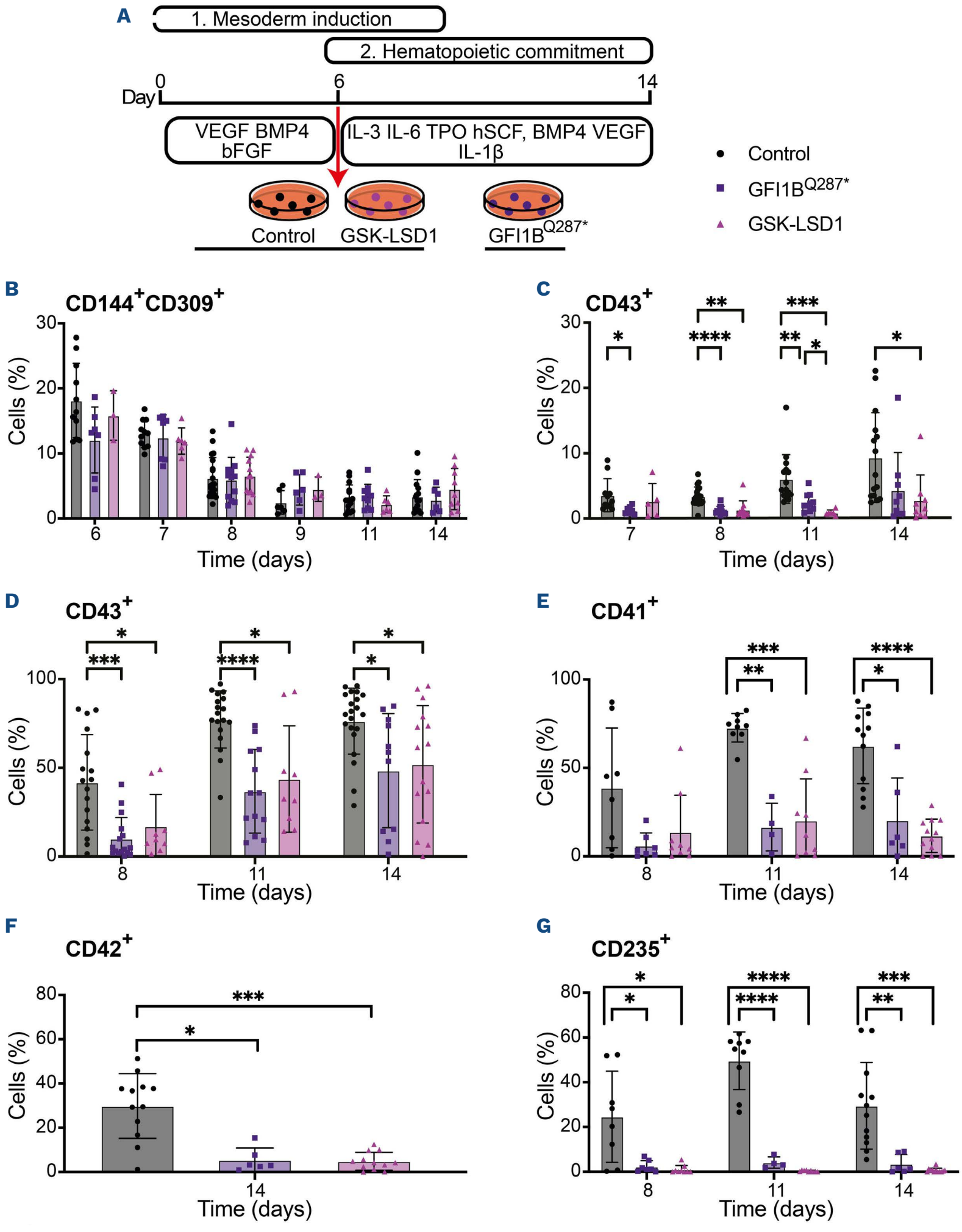

Continued on following page.

Figure 3. LSD1/KDM1A and GFI1B are critical regulators governing endothelial-to-hematopoietic transition from induced pluripotent stem cells. (A) Schematic overview of induced pluripotent stem cell (iPSC) differentiation detailing growth factors, induction stages, and the pulse addition of GSK-LSD1 over the timeline in days. (B) Colonies differentiated for 6-14 days were harvested and stained for CD144 and CD309. Frequency of cells double positive for these markers is shown (N=6-20 for control, 6-12 for *GFI1B* Q287*, and 3-12 for GSK-LSD1). (C) Percentage of CD43$^+$ cells within the differentiated colonies (N=11-20 for control, 7-12 for *GFI1B* Q287*, and 5-11 for GSK-LSD1). (D) Early hematopoietic commitment was evaluated by assessing the proportion of CD43$^+$ cells among suspension cells during the differentiation of iPSC (N=17-21 for control, 11-16 for *GFI1B* Q287*, and 9-15 for GSK-LSD1). (E) The frequency of CD41$^+$ megakaryocytic/early hematopoietic progenitors (N=8-12 for control, 4-7 for *GFI1B* Q287*, and 9-12 for GSK-LSD1), (F) CD42$^+$ megakaryocytic (N=12 for control, 6 for *GFI1B* Q287*, and 12 for GSK-LSD1) and (G) CD235$^+$ erythroid (N=8-12 for control, 4-7 for *GFI1B* Q287*, and 9-12 for GSK-LSD1) among suspension cells during iPSC colony differentiation, in the absence or presence of GSK-LSD1, or in cultures of iPSC carrying the *GFI1B* Q287* mutation. (B-G) Data represent mean +/- standard deviation, analyzed using two-way ANOVA, Tukey's multiple comparisons test. Significance levels: *P<0.05, **P<0.005, ***P<0.0005, ****P<0.00005. Representations: black circles = control iPSC; red triangles = iPSC treated with GSK-LSD1 inhibitor; purple squares = *GFI1B* Q287* iPSC.

harvested from the supernatant. In the supernatant fraction from both *GFI1B* Q287* and GSK-LSD1 treated conditions, there was a decline in cell yield (*Online Supplementary Figure S1C, D*), and a noticeable decrease in the proportion of hematopoietic progenitors, as indicated by CD43 and CD41 expression (Figure 3D). Within the reduced hematopoietic compartment, megakaryocytic commitment was drastically decreased in both conditions, as determined by CD41 and CD42 expression (Figure 3E, F). Additionally, an almost complete absence of CD235$^+$ erythroid compartment was observed (Figure 3G). The data indicate that GFI1B and LSD1/KDM1A are crucial modulators during iPSC-EHT and that the progression toward hematopoietic cells and specifically to the megakaryocytic and erythroid lineages depends on their function.

Single-cell RNA sequencing reveals induced pluripotent stem cell-derived hemogenic endothelium and transitional stages to endothelial and hematopoietic cells

Our results suggest that LSD1/KDM1A and GFI1B play a key role in balancing CD144$^+$CD309$^+$ commitment toward either hematopoietic or endothelial fates. The specific stage at which LSD1/KDM1A and GFI1B exert their functions during iPSC-EHT remains unclear. In order to delve deeper into their role at the single cell level, we performed single-cell RNA sequencing (scRNAseq). A control iPSC line was differentiated and subsequently treated with a single pulse of GSK-LSD1 at day 5.[37,46] We then sorted CD144$^+$ and CD31$^+$ cells at day 8, post hematopoietic commitment (Figure 4A). This allowed us to capture both the CD43$^+$ hematopoietic (18.40+/-5.16%) and CD73$^+$ endothelial (46.76+/-11.88%) commitment (*Online Supplementary Figure S1E*). UMAP dimensional reduction revealed five major distinct cell populations, clusters I and II (endothelial), III (hematopoietic), IV (neuronal), and V (lymphoid), with potential transition stages between clusters I-II-III (Figure 4B). We grouped differentially expressed genes into modules (*Online Supplementary Figure S2A, B*) and used genes from each module to determine cell identity (*Online Supplementary Table S2A*). Through this methodology, we pinpointed a total of 11 modules, where genes from modules 3, 5, 8, 9, 10, and 11 reflected the cluster identity (*Online Supplementary Figure S2A, B; Online Supplementary Table S2B*). We performed differential gene expression using linear regression model followed by GSEA between clusters II and III, which showed downregulation of hematopoietic and upregulation of endothelial signatures in cluster II (Figure 4C; *Online Supplementary Table S2C, D*). We also noticed an enriched hematopoietic stem cell signature in cluster II (*Online Supplementary Figure S2C; Online Supplementary Table S2E*). Comparing cluster II to cluster I, GSEA showed upregulation of hematopoietic and downregulation of endothelial signatures in cluster II (*Online Supplementary Figure S2D; Online Supplementary Table S2F, G*). Together, these steps characterized cluster II as iPSC-HE. Top markers from each cluster aligned with the identified cell types (Figure 4D; *Online Supplementary Figures S3, S4*). Lymphoid markers CD3 and CD7 were exclusively found in the lymphoid cluster (V; *Online Supplementary Figures S3, S4*). An embryonic and neuronal specific transcription factor, *SOX2*, and a central nervous system specific receptor protein tyrosine phosphatase, *PTPRZ1*, were uniquely expressed in the neuronal cluster (IV; *Online Supplementary Figures S3, S4*). The endothelial cluster (I) displayed high expression of *TGFB* and its downstream target, *HAND1*, suggesting an endothelial-to-mesenchymal transition of cultured endothelial cells from iPSC (Figure 4D; *Online Supplementary Figures S3, S4*).[51] This could elucidate the significant enrichment of genes encoding cell adhesion and extracellular matrix proteins, including *COL3A1, FN1, ITGA1, IGFBP3, IGFBP7*, and *LUM* (Figure 4D; *Online Supplementary Figures S3, S4*).[51,52] *CD73* was predominantly detected in the endothelial cluster (I; Figure 4D), while hematopoietic markers, such as *CD43, CD41*, and *CD235*, along with transcription factors *KLF1, SPI1, GATA1, GATA2, RUNX1, GFI*, and *GFI1B*, were confined to the hematopoietic cluster (III; Figure 4D; *Online Supplementary Figures S3, S4*). The expression of *CD144, CD31, CD309, CD34*, and other known arterial/hemogenic endothelial markers such as *GJA4, SOX17, DLL4*, and *CD40*, were specifically enriched in the iPSC-HE cluster (II; Figure 4D; *Online Supplementary Figures S3, S4*).[48,53,54] Thus, our scRNAseq data revealed iPSC-HE, committed hematopoietic and endothelial cells, and their transition states.

Trajectory analysis reveals gene regulation dynamics during endothelial-to-hematopoietic transition from induced pluripotent stem cell

Next, we conducted a trajectory analysis to better understand the differentiation process. By designating the endothelial population as the originating node (cluster I; Figure 4B), we computed and established the dynamics of similarity in pseudotime (Figure 5A). Notably, the tra-

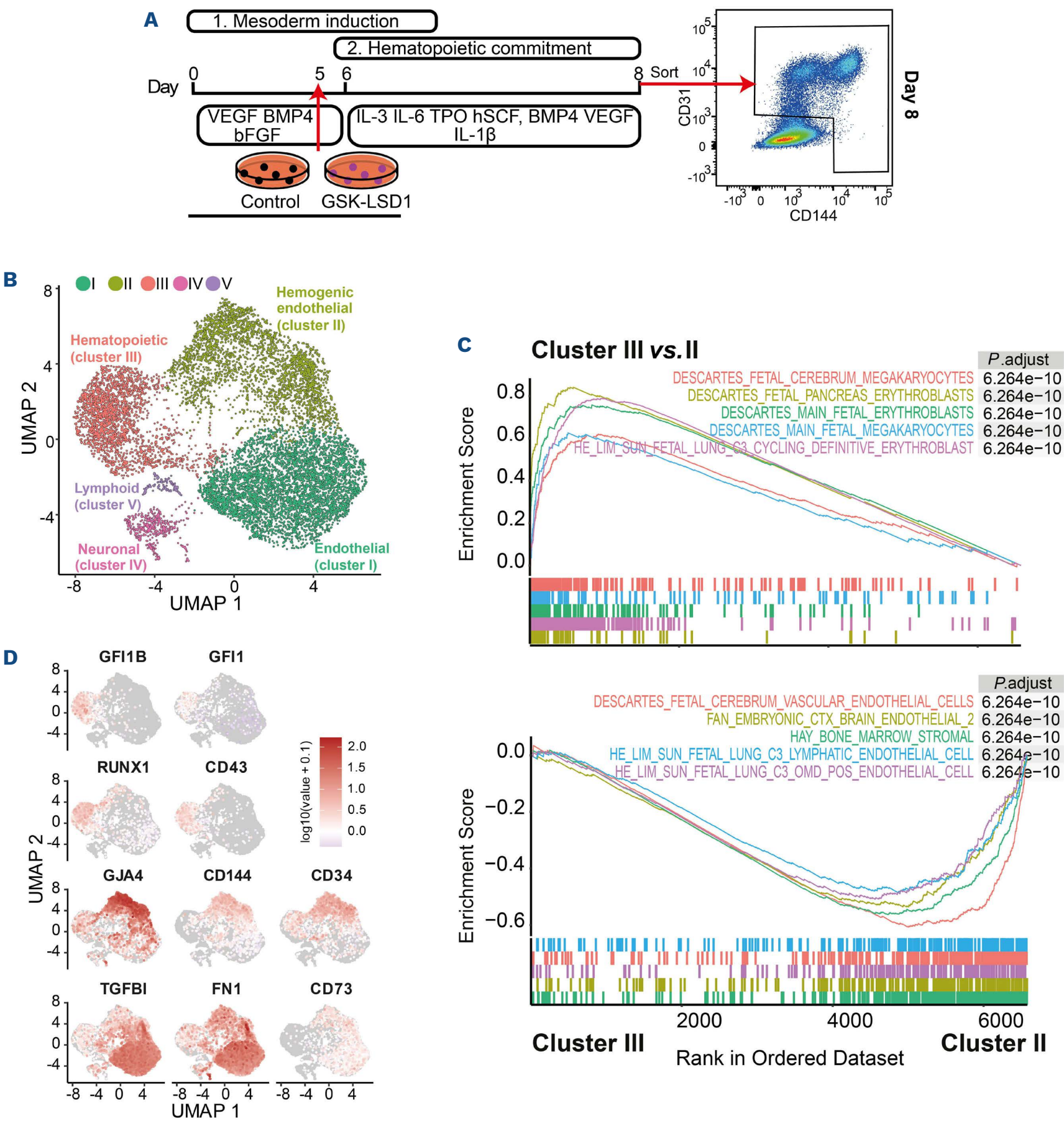

Figure 4. Identification of CD144⁺/CD31⁺ populations using single-cell RNA sequencing. (A) A schematic diagram illustrating the timeline of induced pluripotent stem cell (iPSC) differentiation, specifying the growth factors, induction stages, and the pulse addition of GSK-LSD1. iPSC colonies differentiated by day 8 were stained for CD144 and CD31, and cells positive for either one or both markers were sorted (CD144⁺/CD31⁺). (B) Identification of CD144⁺/CD31⁺ cell populations using UMAP dimensional reduction is displayed, with colors corresponding to the identified cell types. (C) Enrichment of hematopoietic cell types in cluster III (top plot) and endothelial cell types in cluster II (bottom plot) by gene set enrichment analysis (GSEA). (D) Uniform manifold approximation and projection (UMAP) plots displaying the expression of hematopoietic genes (*GFI1B, GFI1, RUNX1, CD43*), hemogenic endothelium (HE)-associated genes (*GJA4, CD144, CD34*), and endothelial-related genes (*TGFBI, FN1, CD73*).

jectory linking the iPSC-HE to both the hematopoietic and the endothelial clusters showed a reduction in the number of cells during transitional phases. This reduction was especially profound during the hematopoietic transition state, suggesting limited cellular proliferation during this phase. The pseudotime trajectory also allowed us to plot transcript abundance from iPSC-HE through iPSC-EHT to hematopoietic committed cells. We focused on the transcripts associated with *in vivo* AGM-EHT, including *NOTCH1, DLL4, HOXA5, HOXA9, ERG, LCOR, GATA2, RUNX1, SPI1, GFI1*, and *GFI1B* (Figure 5B; *Online Supplementary Figure S5A, B*). The expression of *NOTCH1* and its ligand, *DLL4*, increased in iPSC-HE and decreased during iPSC-EHT (Figure 5B; *Online Supplementary Figure S4*). This trend was followed by the upregulation of hematopoietic transcription factors such as *GATA2, RUNX1, GFI1,* and *GFI1B* (Figure 4D; Figure 5B; *Online Supplementary Figure S4*). While *GFI1B* expression was not detected in iPSC-HE, it was upregulated during iPSC-EHT following the upregulation of *GATA2* and *RUNX1*. *LSD1/KDM1A*, a co-factor of GFI1B, was ubiquitously expressed (Figure 5C; *Online Supplementary Figure S5C*). Other known co-factors of GFI1B, such as *RCOR1, HDAC1*, and *HDAC2*, were also present in the iPSC-HE (Figure 5C; *Online Supplementary Figure S5C*). The trajectory analysis unveiled gene expression dynamics during EHT, pinpointing the absence of *GFI1B* in iPSC-HE and ubiquitous expression of *LSD1/KDM1A*.

LSD1/KDM1A is essential for edothelial-to-hematopoietic transition of induced pluripotent stem cell-derived hemogenic endothelium and is involved in endothelial differentiation

Next, we assessed the impact of GFI1B's co-factor LSD1/KDM1A on iPSC-HE specification toward hematopoietic or endothelial lineages through inhibition using GSK-LSD1. Inhibition of LSD1/KDM1A resulted in the absence of the

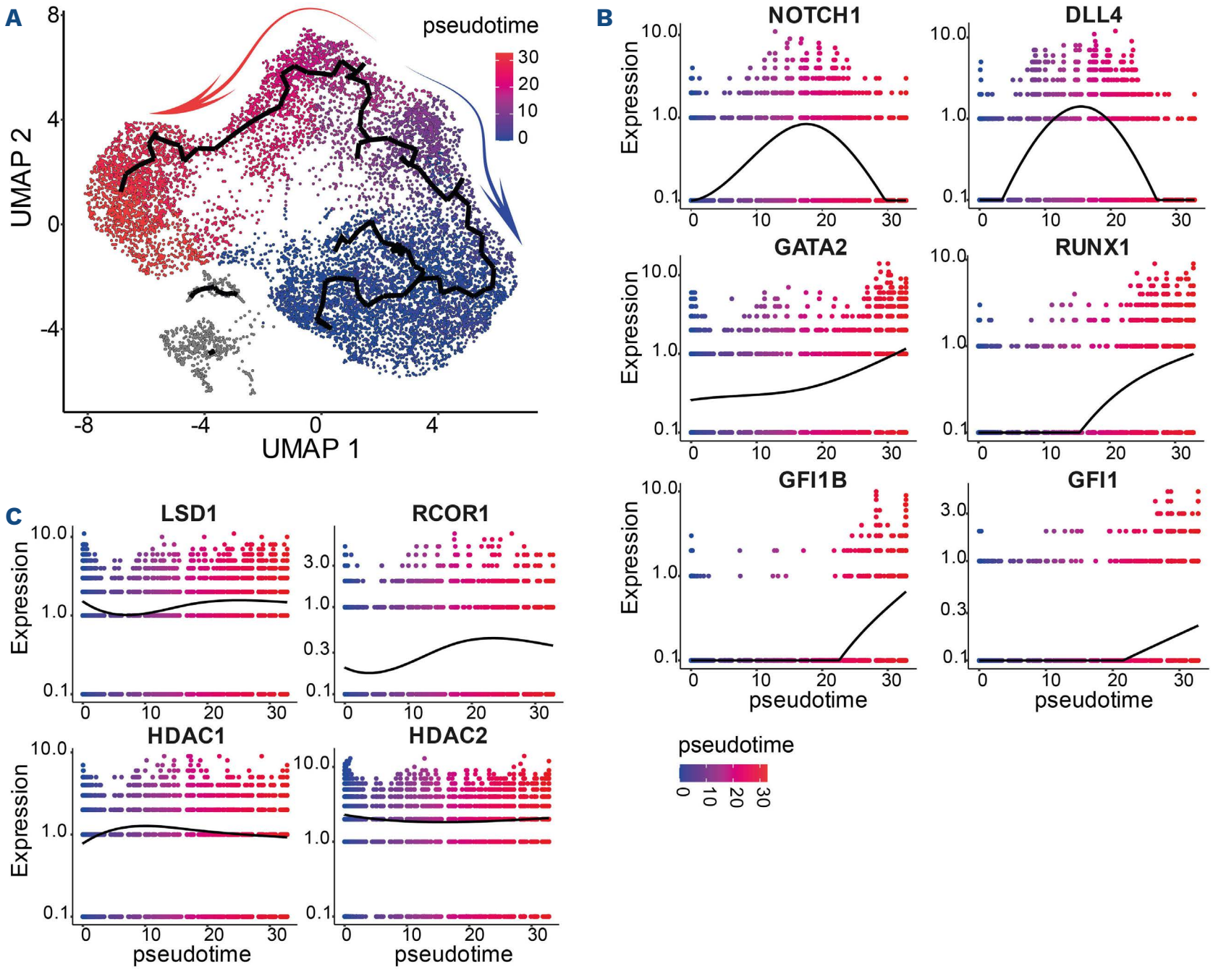

Figure 5. Pseudotime gene expression analysis during endothelial-to-hematopoietic transition from induced pluripotent stem cell. (A) UMAP visualization of cells along the pseudotime, with the inferred pseudotime represented by a color gradient from blue to red. (B) Expression of *NOTCH1, DLL4, GATA2, RUNX1, GFI1B*, and *GFI* over pseudotime. (C) Expression of GFI1B co-factors, *LSD1/KDM1A, RCOR1, HDAC1*, and *HDAC2* over pseudotime.

hematopoietic cluster (Figure 6A, B; *Online Supplementary Figure S6*). This finding aligns with the suppression of hematopoietic commitment by GSK-LSD1 as shown in Figure 3. At the same time, LSD1/KDM1A inhibition did not impede differentiation into the endothelial lineage (Figure 6B; *Online Supplementary Figure S6*). This was also validated by the expression of endothelial markers using flow cytometry (*Online Supplementary Figure S1B*). However, the endothelial populations differentiated in the presence or absence of GSK-LSD1 did not fully overlap (Figure 6A), suggesting that LSD1/KDM1A inhibition also influences the gene expression program during endothelial differentiation/specification. In summary, our scRNAseq data demonstrated that LSD1/KDM1A inhibition results in an early block of EHT preceding the evident expression of *GFI1B*. This indicates that while the phenotypes of *GFI1B* Q287* mutation and GSK-LSD1 might appear similar based on marker expression, they likely can exert their effects at different cellular states.

Ectopic expression of GFI1B in hemogenic endothelium suppresses endothelial and activates hematopoietic programs

Considering that LSD1/KDM1A is a co-factor of GFI1B, and its inhibition leads to a block of EHT, we hypothesized that the ectopic expression of GFI1B in iPSC-HE might result in a converse effect, specifically reinforcing the hematopoietic fate and downregulating the endothelial gene expression profile. We generated an additional scRNAseq dataset from the same experiment but at day 5 (prior to hematopoietic or endothelial specification) of differentiation and integrated it with the day 8 scRNAseq dataset (*Online Supplementary Figure S7A*). We observed a ubiquitous expression of *LSD1/KDM1A*, whereas GFI1B was not detected prior to hematopoietic commitment (*Online Supplementary Figure S7B*). We then lentivirally transduced GFI1B into day 5 sorted $CD34^+CD144^+CD31^+CD43^-CD73^-$ cells (Figure 7A) and allowed them to differentiate further into $CD73^+$ endothelial or $CD43^+$ hematopoietic cells. More than 95% of the cells were GFP-positive 5 days after transduction (*Online Supplementary Figure S7C*). GFI1B ectopic expression led to an increase in the total number of cells and in the number of $CD73^+$ cells (*Online Supplementary Figure S7D, E*). Flow cytometry revealed a reduction in the endothelial marker CD73 and a slight decrease in the hematopoietic marker CD43 expression (Figure 7A, B). We then investigated transcriptional differences between the two groups using bulk RNA sequencing. Principal component (PC) analysis showed a clear segregation of the GFI1B overexpressed conditions from the empty vector controls (*Online Supplementary Figure S8A*), with PC1 explaining 76% of the variance. We identified 846 upregulated and 446 downregulated genes in the GFI1B overexpressed samples (Figure 7C; *Online Supplementary Table S3A*). As expected, *GFI1B* was among the top 10 differentially expressed genes (*Online Supplementary Figure S8B; Online Supplementary Table S3A*). Gene ontology terms related to cell cycle were significantly upregulated, aligning with the increased cell numbers (*Online Supplementary Figure S7D; Online Supplementary Table S3B*). Gene set enrichment analysis manifested a potent reduction of the endothelial signature and a robust upregulation of the hematopoietic signature (Figure 7D; *Online Supplementary Table S3C*). Upregulated genes included *GATA2, RUNX1, KIT, CD43*, while downregulated genes comprised

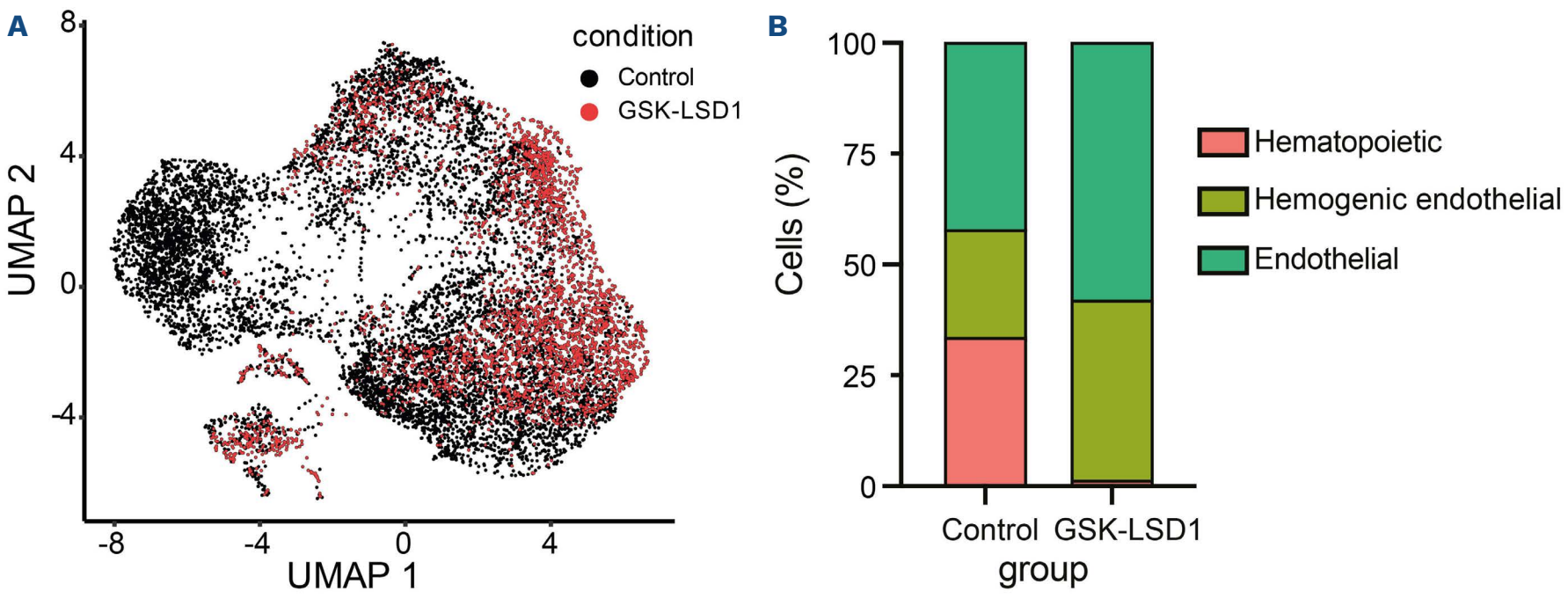

Figure 6. GSK-LSD1 blocks endothelial-to-hematopoietic transition from induced pluripotent stem cell. (A) Uniform manifold approximation and projection (UMAP) visualization of single $CD31^+/CD144^+$ cells differentiated from an induced pluripotent stem cell (iPSC) line derived from a healthy donor, displayed under both untreated control (black) and GSK-LSD1 treated conditions (red). (B) Proportional representation of hematopoietic, hemogenic endothelial (HE), and endothelial populations, presented in Figure 5B, under both control and GSK-LSD1 conditions (control: hematopoietic 0.324, HE 0.257, endothelial 0.419; GSK-LSD1: hematopoietic 0.015, HE 0.394, endothelial 0.591).

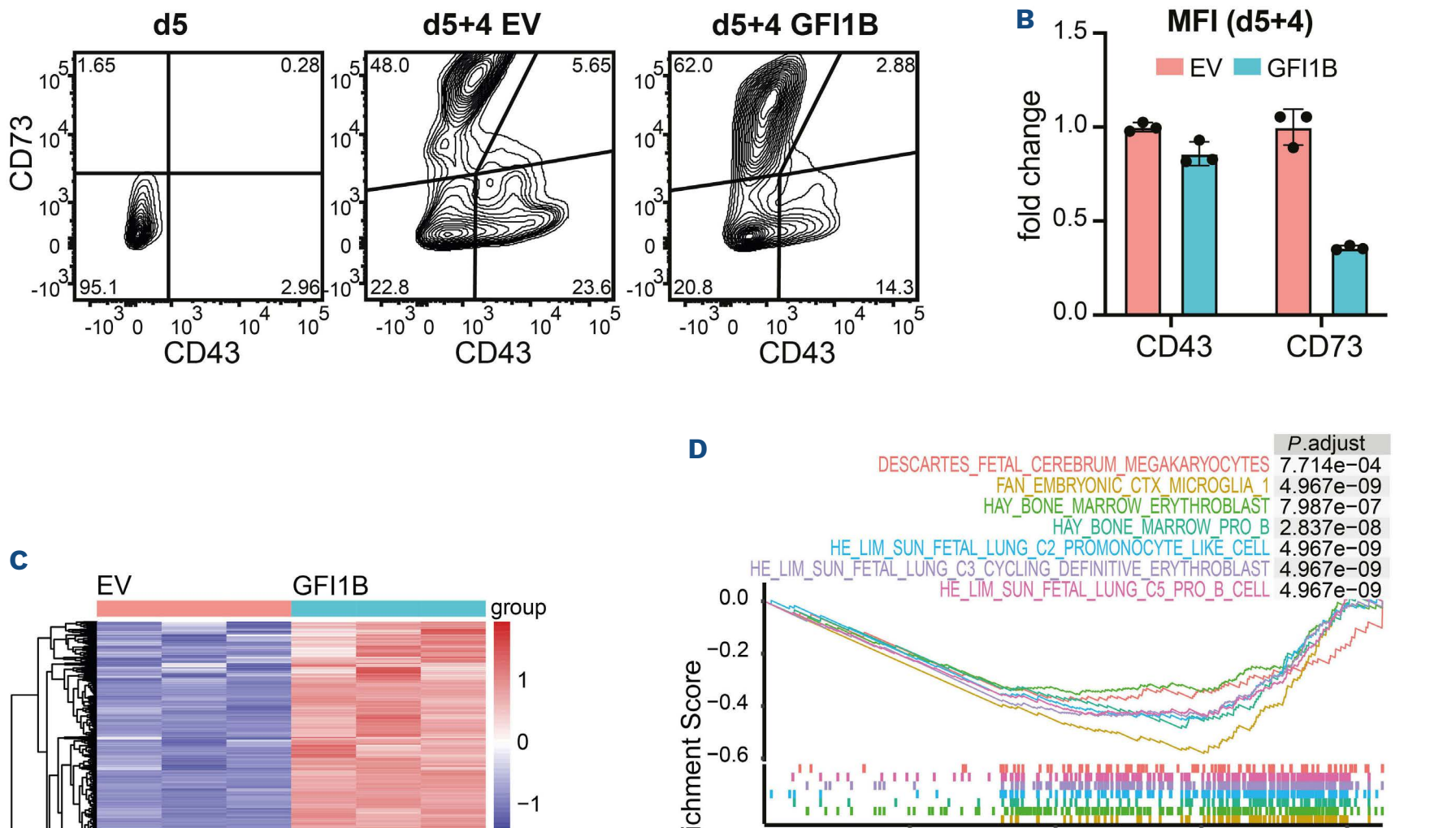

Figure 7. GFI1B ectopic expression in induced pluripotent stem cell-derived hemogenic endothelium leads to upregulation of hematopoietic genes and downregulation of endothelial genes. (A) Flow cytometry analysis of the endothelial marker CD73 and the hematopoietic marker CD43 on day 0 and day 4 following transduction with either empty vector (EV) or GFI1B. The percentages are indicated within the plot. (B) Comparison of mean fluorescence intensity (MFI) of CD43 and CD73 on day 4 post-transduction between EV and GFI1B groups (N=3; mean +/- standard deviation; analyzed via Mann-Whitney test; *P*=0.1 for both). (C) Heatmap displaying differentially expressed genes between EV and GFI1B groups on day 4 following transduction. (D) Enrichment of hematopoietic cell types in GFI1B-overexpressed induced pluripotent stem cell (iPSC)-hemogenic endothelium (HE) (top plot) and endothelial cell types in EV (bottom plot) by gene set enrichment analysis (GSEA).

CD73, SOX6, SOX14, and *SOX17* (*Online Supplementary Figure S8C*; *Online Supplementary Table S3A*). *HOXA9* and *HOXA10* were lowly expressed, while *HOXA5* remained undetected (*Online Supplementary Figure S8C*). *GFI1*, on the other hand, was decreased by GFI1B overexpression (*Online Supplementary Figure S8C*). Consequently, GFI1B overexpression promotes a hematopoietic program at the expense of an endothelial program, even before the onset of *RUNX1* and *GATA2* expression.

Discussion

Thus far, attempts to derive long-term repopulating hematopoietic stem cells or effector cells from iPSC differentiation *in vitro* have been unsuccessful. *In vivo*, definitive hematopoiesis requires an EHT from the HE in the aorta-gonad-mesonephros (AGM) region of the embryo. In this study, we examined how functional inhibition of GFI1B and LSD1/KDM1A impacts the generation of iPSC-HE and the process

of iPSC-EHT. We used patient-derived iPSC lines harboring a heterozygous mutation in *GFI1B* (*GFI1B* Q287*) and inhibited LSD1/KDM1A in healthy iPSC lines using GSK-LSD1. Treatment of iPSC differentiated toward the hematopoietic lineage with GSK-LSD1, or hematopoietic differentiation of *GFI1B* Q287* mutant iPSC, did not impair iPSC-HE formation. However, hematopoietic lineage commitment was profoundly impaired. Patients with heterozygous *GFI1B* Q287* mutation manifested thrombocytopenia,[50] so it is unlikely that GFI1B/LSD1 inhibition blocks the proliferation of early hematopoietic progenitors. Indeed, although GFI1B-deficient mice die prenatally at E15 due to a severe defect in erythropoiesis and megakaryopoiesis, conditional deficiency for Gfi1b in adult mice allows HSC to maintain self-renewal and multilineage differentiation capabilities despite increased levels of reactive oxygen species and loss of quiescence.[55] Of note, this hematopoietic ablation does lead to defects in erythropoiesis and megakaryopoiesis in adult mice,[56] and a myeloid bias in iPSC differentiation.[57] Furthermore, LSD1 inhibition leads to expansion of human hematopoietic progenitors *in vitro*.[58] Treatment with GSK-LSD1 resulted in a complete absence of EHT from iPSC-HE and a subsequent lack of hematopoietic cells, indicating a crucial dependence of iPSC-derived hematopoiesis on LSD1/KDM1A. This finding aligns with previous research showing that Lsd1/LSD1 inhibition blocks EHT in *ex vivo* cultured mouse AGM explants and prevents embryoid body differentiation in both RUNX1^{-} primitive and RUNX1^{+} definitive hematopoiesis.[35,59] Additionally, these results corroborate the essential role of Lsd1's binding partner, Gfi1b (and Gfi1), in the emergence of hematopoietic cells from these isolated intra-aortic hematopoietic clusters.[25,35] Collectively, this indicates that iPSC-derived hematopoiesis similarly depends on LSD1/GFI1B. Interestingly, the block in hematopoietic commitment induced by GSK-LSD1 preceded the upregulation of *GFI1* and *GFI1B*. This suggests different and temporally distinct roles for LSD1/KDM1A during EHT, the first of which may not rely on GFI1B/GFI1. Our data illustrate that GFI1B and LSD1/KDM1A are crucial regulators of the hematopoietic commitment of iPSC-HE via EHT.

Through trajectory analysis in pseudotime, we confirmed that the expression of key EHT regulators during iPSC-EHT, such as *NOTCH1, RUNX1*, and *GFI1B*, shares similar kinetics to those of the *in vivo* EHT. Our data probably mimics extraembryonic definitive hematopoiesis given lack of *HOXA* expression.[60] Sugimura *et al*. compared iPSC-HE with fetal liver hematopoiesis in mice and humans and identified nine genes differentially expressed and required for long-term repopulating HSPC capability, specifically *ERG, HOXA5, HOXA9, HOXA10, LCOR, RUNX1*, and *SPI1*.[17] Overexpression of these genes in iPSC-HE followed by injection into mice led to long-term reconstitution, albeit low engraftment levels.[17] However, it remains unclear whether the ectopic expression of GFI1B alone in iPSC-derived HE can drive EHT in human hematopoiesis. While GFI1B primarily functions as a transcriptional repressor, ectopic expression in HE resulted in 846 upregulated and 446 downregulated genes, suggesting dual roles for GFI1B as both a transcriptional activator and repressor.[31] However, the precise relationship between these differentially expressed genes and GFI1B, whether direct or indirect, remains to be elucidated. Importantly, upregulated genes are enriched for hematopoietic specification, while downregulated genes are associated with endothelial specification. Notably, the hematopoietic transcription factors *RUNX1* and *GATA2* were among the upregulated genes. GFI1B is recognized as a downstream target of RUNX1. In mouse embryonic stem cells that lack Runx1, Gfi1b aids in differentiation toward hematopoietic cells during EHT by suppressing endothelial and promoting hematopoietic programs.[61] A recent study observed diminished Gfi1b expression in *Gata2*$^{+/-}$ mice HSC and demonstrated Gfi1b's capacity to restore embryonic HSC in *gata2b*$^{-/-}$ zebrafish.[22] Our dataset also suggests that GFI1B can function both upstream and downstream of RUNX1 and GATA2 during iPSC-EHT, directing HE to the hematopoietic fate. We observed a decrease in *GFI1* expression by forced GFI1B overexpression, which agreed with previous finding that GFI1/GFI1B repress *GFI1* expression in human T cells.[62] We speculate that the reason why we did not observe an increased CD43 membrane expression might be due to the specific transcriptional regulation of CD43-associated proteins, which could be independent of GFI1B.

Purified iPSC-derived CD144^{+}CD31^{+}CD34^{+} cells tend to differentiate more toward the endothelial lineage than the hematopoietic lineage. Although these cells are non-committed, i.e., CD43^{-}CD73^{-}, a bias toward endothelial differentiation cannot be excluded. However, CD144^{+}CD31^{+}CD34^{+} cells, prior to specification, did not reveal any clearly separated populations based on RNA expression profiles (*Online Supplementary Figure S7A*). Ectopic GFI1B expression suggests a conflicted state between differentiating into hematopoietic or endothelial lineages. Indeed, GFI1B expression in iPSC-HE by itself was insufficient to drive EHT but did provide a clear singular transcriptional program initiated by this transcription factor. It becomes important to perform similar experiments with other regulators of EHT, and by comparing our single-cell data to *in vitro* and *in vivo* studies of fetal hematopoiesis.

In conclusion, the roles of LSD1/KDM1A and GFI1B during *in vitro* EHT are critical for iPSC-derived hematopoiesis. While both the dominant-negative mutation of *GFI1B* (*GFI1B* Q287*) and LSD1/KDM1A inhibition obstruct EHT, LSD1/KDM1A can probably operate at distinct temporal points that are either dependent or independent on GFI1/GFI1B and in different cellular subsets. Furthermore, ectopic expression of GFI1B in HE cells results in the downregulation of endothelial genes and upregulation of hematopoietic genes. The precisely timed expression of specific transcriptional regulators during EHT appears to be important to the eventual outcome of EHT.

Disclosures
No conflicts of interest to disclose.

Contributions
HZ, MH, and FdS performed the experiments. HZ, MH, and EvdA designed the experiments, analyzed the data, and wrote the manuscript. NG performed the RNA isolation and sequencing. HZ, MH, WFJvIJ, and AS analyzed the RNA sequencing data. MvL, SP, BvdR, and EV contributed to the experimental design and the writing of the manuscript. All authors critically revised the manuscript.

Acknowledgments
The authors are grateful for the assistance provided by the Central Facility of Sanquin with flow cytometry and sorting.

Funding
This work was supported by the Dutch Scientific Research organization (NWO) in the framework of the NWA-ORC Call grant agreement NWA.1160.18.038 (SYMPHONY), and by the ZonMw TRACER consortium as part of the PSIDER program (grant number 10250022110001).

Data-sharing statement
For original data, please contact the corresponding author. Sequencing data are available at GEO under the accession number GSE246386.

References

1. Ivanovs A, Rybtsov S, Ng ES, et al. Human haematopoietic stem cell development: from the embryo to the dish. Development. 2017;144(13):2323-2337.
2. Palis J. Hematopoietic stem cell-independent hematopoiesis: emergence of erythroid, megakaryocyte, and myeloid potential in the mammalian embryo. FEBS Lett. 2016;590(22):3965-3974.
3. Palis J, Robertson S, Kennedy M, Wall C, Keller G. Development of erythroid and myeloid progenitors in the yolk sac and embryo proper of the mouse. Development. 1999;126(22):5073-5084.
4. Frame JM, McGrath KE, Palis J. Erythro-myeloid progenitors: "definitive" hematopoiesis in the conceptus prior to the emergence of hematopoietic stem cells. Blood Cells Mol Dis. 2013;51(4):220-225.
5. McGrath KE, Frame JM, Fegan KH, et al. Distinct sources of hematopoietic progenitors emerge before HSCs and provide functional blood cells in the mammalian embryo. Cell Rep. 2015;11(12):1892-1904.
6. Lassila O, Martin C, Toivanen P, Dieterlen-Lievre F. Erythropoiesis and lymphopoiesis in the chick yolk-sac-embryo chimeras: contribution of yolk sac and intraembryonic stem cells. Blood. 1982;59(2):377-381.
7. De Bruijn MFTR, Speck NA, Peeters MCE, Dzierzak E. Definitive hematopoietic stem cells first develop within the major arterial regions of the mouse embryo. EMBO J. 2000;19(11):2465-2474.
8. De Bruijn MFTR, Ma X, Robin C, et al. Hematopoietic stem cells localize to the endothelial cell layer in the midgestation mouse aorta. Immunity. 2002;16(5):673-683.
9. Medvinsky A, Dzierzak E. Definitive hematopoiesis is autonomously initiated by the AGM region. Cell. 1996;86(6):897-906.
10. Ivanovs A, Rybtsov S, Welch L, et al. Highly potent human hematopoietic stem cells first emerge in the intraembryonic aorta-gonad-mesonephros region. J Exp Med. 2011;208(12):2417-2427.
11. Frame JM, Fegan KH, Conway SJ, McGrath KE, Palis J. Definitive hematopoiesis in the yolk sac emerges from Wnt-responsive hemogenic endothelium independently of circulation and arterial identity. Stem Cells. 2016;34(2):431-444.
12. Yoshimoto M, Porayette P, Glosson NL, et al. Autonomous murine T-cell progenitor production in the extra-embryonic yolk sac before HSC emergence. Blood. 2012;119(24):5706-5714.
13. Yoshimoto M, Montecino-Rodriguez E, Ferkowicz MJ, et al. Embryonic day 9 yolk sac and intra-embryonic hemogenic endothelium independently generate a B-1 and marginal zone progenitor lacking B-2 potential. Proc Natl Acad Sci U S A. 2011;108(4):1468-1473.
14. Boisset JC, Van Cappellen W, Andrieu-Soler C, et al. In vivo imaging of haematopoietic cells emerging from the mouse aortic endothelium. Nature. 2010;464(7285):116-120.
15. Lacaud G, Kouskoff V. Hemangioblast, hemogenic endothelium, and primitive versus definitive hematopoiesis. Exp Hematol. 2017;49:19-24.
16. Suzuki N, Yamazaki S, Yamaguchi T, et al. Generation of engraftable hematopoietic stem cells from induced pluripotent stem cells by way of teratoma formation. Mol Ther. 2013;21(7):1424-1431.
17. Sugimura R, Jha DK, Han A, et al. Haematopoietic stem and progenitor cells from human pluripotent stem cells. Nature. 2017;545(7655):432-438.
18. Möröy T, Vassen L, Wilkes B, Khandanpour C. From cytopenia to leukemia: the role of Gfi1 and Gfi1b in blood formation. Blood. 2015;126(24):2561-2569.
19. Saleque S, Cameron S, Orkin SH. The zinc-finger proto-oncogene Gfi-1b is essential for development of the erythroid and megakaryocytic lineages. Genes Dev. 2002;16(3):301-306.
20. Tsai FY, Keller G, Kuo FC, et al. An early haematopoietic defect in mice lacking the transcription factor GATA-2. Nature. 1994;371(6494):221-226.
21. de Pater E, Kaimakis P, Vink CS, et al. Gata2 is required for HSC generation and survival. J Exp Med. 2013;210(13):2843-2850.
22. Koyunlar C, Gioacchino E, Vadgama D, et al. Gata2-regulated Gfi1b expression controls endothelial programming during endothelial-to-hematopoietic transition. Blood Adv. 2023;7(10):2082-2093.
23. North T, Gu TL, Stacy T, et al. Cbfa2 is required for the formation of intra-aortic hematopoietic clusters. Development. 1999;126(11):2563-2575.
24. Wang Q, Stacy T, Binder M, et al. Disruption of the Cbfa2 gene causes necrosis and hemorrhaging in the central nervous system and blocks definitive hematopoiesis. Proc Natl Acad Sci U S A. 1996;93(8):3444-3449.
25. Thambyrajah R, Patel R, Mazan M, et al. New insights into the regulation by RUNX1 and GFI1(s) proteins of the endothelial to hematopoietic transition generating primordial hematopoietic cells. Cell Cycle. 2016;15(16):2108-2114.

26. Anguita E, Villegas A, Iborra F, Hernández A. GFI1B controls its own expression binding to multiple sites. Haematologica. 2010;95(1):36-46.
27. Chiang C, Ayyanathan K. SNAIL/Gfi-1 (SNAG) family zinc finger proteins in transcription regulation, chromatin dynamics, cell signaling, development, and disease. Cytokine Growth Factor Rev. 2013;24(2):123-131.
28. Saleque S, Kim J, Rooke HM, Orkin SH. Epigenetic regulation of hematopoietic differentiation by Gfi-1 and Gfi-1b is mediated by the cofactors CoREST and LSD1. Mol Cell. 2007;27(4):562-572.
29. Zweidler-Mckay PA, Grimes HL, Flubacher MM, Tsichlis PN. Gfi-1 encodes a nuclear zinc finger protein that binds DNA and functions as a transcriptional repressor. Mol Cell Biol. 1996;16(8):4024-4034.
30. Duan Z, Horwitz M. Targets of the transcriptional repressor oncoprotein GFI-1. Proc Natl Acad Sci U S A. 2003;100(10):5932-5937.
31. Acar M, Jafar-Nejad H, Giagtzoglou N, et al. Senseless physically interacts with proneural proteins and functions as a transcriptional co-activator. Development. 2006;133(10):1979-1989.
32. Wang J, Scully K, Zhu X, et al. Opposing LSD1 complexes function in developmental gene activation and repression programmes. Nature. 2007;446(7138):882-887.
33. Sprüssel A, Schulte JH, Weber S, et al. Lysine-specific demethylase 1 restricts hematopoietic progenitor proliferation and is essential for terminal differentiation. Leukemia. 2012;26(9):2039-2051.
34. Takeuchi M, Fuse Y, Watanabe M, et al. LSD1/KDM1A promotes hematopoietic commitment of hemangioblasts through downregulation of Etv2. Proc Natl Acad Sci U S A. 2015;112(45):13922-13927.
35. Thambyrajah R, Mazan M, Patel R, et al. GFI1 proteins orchestrate the emergence of haematopoietic stem cells through recruitment of LSD1. Nat Cell Biol. 2015;18(1):21-32.
36. Wang J, Hevi S, Kurash JK, et al. The lysine demethylase LSD1 (KDM1) is required for maintenance of global DNA methylation. Nat Genet. 2008 41:1. 2008;41(1):125-129.
37. Hansen M, Varga E, Aarts C, et al. Efficient production of erythroid, megakaryocytic and myeloid cells, using single cell-derived iPSC colony differentiation. Stem Cell Res. 2018;29:232-244.
38. Heshusius S, Heideveld E, Burger P, et al. Large-scale in vitro production of red blood cells from human peripheral blood mononuclear cells. Blood Adv. 2019;3(21):3337-3350.
39. Trapnell C, Cacchiarelli D, Grimsby J, et al. The dynamics and regulators of cell fate decisions are revealed by pseudotemporal ordering of single cells. Nat Biotechnol. 2014;32(4):381-386.
40. Qiu X, Mao Q, Tang Y, et al. Reversed graph embedding resolves complex single-cell trajectories. Nat Methods. 2017;14(10):979-982.
41. Cao J, Spielmann M, Qiu X, et al. The single-cell transcriptional landscape of mammalian organogenesis. Nature. 2019;566(7745):496-502.
42. McInnes L, Healy J, Melville J. UMAP: uniform manifold approximation and projection for dimension reduction. arXiv. 2020 Sep 18. doi:10.48550/arXiv.1802.03426 [preprint, not peer-reviewed]
43. Blondel VD, Guillaume JL, Lambiotte R, Lefebvre E. Fast unfolding of communities in large networks. J Stat Mech. 2008;2008(10):P10008.
44. Heshusius S, Grech L, Gillemans N, et al. Epigenomic analysis of KLF1 haploinsufficiency in primary human erythroblasts. Sci Rep. 2022;12(1):336.
45. Hansen M, Varga E, Wüst T, et al. Generation and characterization of human iPSC lines SANi001-A and SANi002-A from mobilized peripheral blood derived megakaryoblasts. Stem Cell Res. 2017;25:42-45.
46. Hansen M, Varga E, Wüst T, et al. Generation and characterization of human iPSC line MML-6838-Cl2 from mobilized peripheral blood derived megakaryoblasts. Stem Cell Res. 2017;18:26-28.
47. Choi KD, Vodyanik MA, Togarrati PP, et al. Identification of the hemogenic endothelial progenitor and its direct precursor in human pluripotent stem cell differentiation cultures. Cell Rep. 2012;2(3):553-567.
48. Sturgeon CM, Ditadi A, Clarke RL, Keller G. Defining the path to hematopoietic stem cells. Nat Biotechnol. 2013;31(5):416-418.
49. Van Oorschot R, Hansen M, Koornneef JM, et al. Molecular mechanisms of bleeding disorderassociated GFI1BQ287* mutation and its affected pathways in megakaryocytes and platelets. Haematologica. 2019;104(7):1460-1472.
50. Hansen M, Varga E, Wüst T, et al. Generation and characterization of a human iPSC line SANi005-A containing the gray platelet associated heterozygous mutation p.Q287* in GFI1B. Stem Cell Res. 2017;25:34-37.
51. Wang H, Wang M, Wen Y, et al. Biphasic regulation of mesenchymal genes controls fate switches during hematopoietic differentiation of human pluripotent stem cells. Adv Sci. 2020;7(20):2001019.
52. Angelos MG, Abrahante JE, Blum RH, Kaufman DS. Single cell resolution of human hemato-endothelial cells defines transcriptional signatures of hemogenic endothelium. Stem Cells. 2018;36(2):206-217.
53. Zeng Y, He J, Bai Z, et al. Tracing the first hematopoietic stem cell generation in human embryo by single-cell RNA sequencing. Cell Res. 2019;29(11):881-894.
54. Pearson S, Lancrin C, Lacaud G, Kouskoff V. The sequential expression of CD40 and Icam2 defines progressive steps in the formation of blood precursors from the mesoderm germ layer. Stem Cells. 2010;28(6):1089-1098.
55. Khandanpour C, Sharif-Askari E, Vassen L, et al. Evidence that Growth factor independence 1b regulates dormancy and peripheral blood mobilization of hematopoietic stem cells. Blood. 2010;116(24):5149-5161.
56. Foudi A, Kramer DJ, Qin J, et al. Distinct, strict requirements for Gfi-1b in adult bone marrow red cell and platelet generation. J Exp Med. 2014;211(5):909-927.
57. Venhuizen J, van Bergen MGJM, Bergevoet SM, et al. GFI1B and LSD1 repress myeloid traits during megakaryocyte differentiation. Commun Biol. 2024;7(1):1-9.
58. Subramaniam A, Žemaitis K, Talkhoncheh MS, et al. Lysine-specific demethylase 1A restricts ex vivo propagation of human HSCs and is a target of UM171. Blood. 2020;136(19):2151-2161.
59. Bruveris FF, Ng ES, Leitoguinho AR, et al. Human yolk sac-like haematopoiesis generates RUNX1-, GFI1- and/or GFI1B- dependent blood and SOX17-positive endothelium. Development. 2020;147(20):dev193037.
60. Ng ES, Azzola L, Bruveris FF, et al. Differentiation of human embryonic stem cells to HOXA+ hemogenic vasculature that resembles the aorta-gonad-mesonephros. Nat Biotechnol. 2016;34(11):1168-1179.
61. Lancrin C, Mazan M, Stefanska M, et al. GFI1 and GFI1B control the loss of endothelial identity of hemogenic endothelium during hematopoietic commitment. Blood. 2012;120(2):314-322.
62. Doan LL, Porter SD, Duan Z, et al. Targeted transcriptional repression of Gfi1 by GFI1 and GFI1B in lymphoid cells. Nucleic Acids Res. 2004;32(8):2508-2519.